

# Anchoring of Tryptophan and Tyrosine Analogs at the Hydrocarbon–Polar Boundary in Model Membrane Vesicles: Parallax Analysis of Fluorescence Quenching Induced by Nitroxide-Labeled Phospholipids<sup>†</sup>

Kelli Kachel, Emma Asuncion-Punzalan, and Erwin London\*

Department of Biochemistry and Cell Biology, State University of New York at Stony Brook,  
Stony Brook, New York 11794-5215

Received August 7, 1995; Revised Manuscript Received September 21, 1995<sup>®</sup>

**ABSTRACT:** The role of Trp and Tyr residues in determining membrane protein structure is particularly interesting because indole and phenol structures combine hydrophobic and polar groups, and it is hard to predict the exact region of the membrane at which their energy would be at a minimum. To determine the depths intrinsically favored by these residues, the locations of membrane-associating Trp and Tyr analogs have been determined using a fluorescence quenching technique able to measure depth at high resolution. They are found to locate at the same depths as Trp and Tyr in membrane proteins, 14–15 Å from the bilayer center, which implies an important role for these residues in aligning membrane proteins in precise relationship to the lipid bilayer.

How different amino acid residues control membrane protein structure is unclear. It has been found that residues with aliphatic hydrocarbon side chains, such as Leu, Ile, and Ala, tend to face the hydrocarbon chain of lipids, and that polar residues are rare in such locations (Deisenhofer & Michel, 1989; Weiss et al., 1991; Landolt-Marticorena et al., 1993). Nevertheless, the extent to which polar residues may be tolerated in positions in membrane proteins that are in contact with the hydrocarbon portion of the lipid bilayer is not yet known. In addition, how the polar headgroup region of lipids interacts with different amino acid residues is also not clear. Trp and Tyr are particularly interesting in this regard as they tend to be localized at a particular depth within the membrane. One striking feature of the few solved membrane protein structures is the localization of Trp and Tyr residues at the boundary between the acyl chain and polar regions of the bilayer (Deisenhofer & Michel, 1989; Weiss et al., 1991; Schabert et al., 1995). An unresolved question is whether this represents the intrinsic low energy depth for Trp and Tyr, or if their location is influenced by other features of protein structure. Recent binding studies have shown that indole does take a location partly exposed to a polar environment in bilayers, but have not specified its exact location (Wimley & White, 1992, 1993). Even less is known about membrane-bound phenol groups.

To define the depth of these groups at a high level of resolution, the location of a series of Trp and Tyr analogs in model membrane vesicles was determined using parallax analysis. In this method, the distance of a fluorescent group from the bilayer center is calculated from the difference in its quenching by phospholipids that carry a nitroxide at different depths within the bilayer (Chattopadhyay & London, 1987; Abrams & London, 1992, 1993). The method has been shown to define membrane depth for a variety of

molecules at the 1–2 Å level of resolution (Abrams & London, 1992, 1993; Abrams et al., 1992; Asuncion-Punzalan & London, 1995), and has been used to determine the structure of membrane-inserted peptides and proteins by several groups (Chung et al., 1992; Jones & Gierasch, 1994; Matsuzaki et al., 1994; Palmer & Merrill, 1994; Rodionova et al., 1995).

## MATERIALS AND METHODS

**Materials.** 1,2-Dioleoyl-*sn*-glycero-3-phosphocholine (DOPC),<sup>1</sup> TPC, 5SLPC, and 12SLPC were purchased from Avanti Polar Lipids. 4-(*tert*-octyl)phenol, 9-methylcarbazole, carbazole, 9-methylanthracene, and anthracene were purchased from Aldrich Chemical. 11-(9-Carbazole)undecanoic acid was purchased from Molecular Probes and IBA from Fluka. Lipid and fatty acid purity was assayed as described previously (Abrams & London, 1992, 1993). Fluorophore purity was checked by melting point. Only carbazole needed further purification by recrystallization. The remaining compounds had melting points at most 1–2 °C below literature values.

**Preparation of Samples for Nitroxide Quenching Experiments.** Samples were prepared by combining in organic solvent 200–250 nmol of lipid with 1 mol % (Trp and anthracene analogs) or 2 mol % (octylphenol) fluorophore. In terms of phospholipid, samples contained either DOPC or a mixture of 85 mol % DOPC and 15 mol % of one of the nitroxide-labeled phosphatidylcholines. For SUV, samples were dried under N<sub>2</sub> and redissolved in 20 µL of ethanol, and 980 µL of buffer was added (10 mM sodium acetate, 150 mM NaCl, pH 5, except in the case of IBA for which measurements were made in 10 mM Gly, 150 mM NaCl, pH 3, to ensure protonation). Most of the compounds in

\* This work was supported by NIH Grant RO1 GM 48596.

\* Address correspondence to this author. Phone: (516) 632-8564. Fax: (516) 632-8575. E-mail: elondon@ccmail.sunysb.edu.

<sup>®</sup> Abstract published in *Advance ACS Abstracts*, November 1, 1995.

<sup>1</sup> Abbreviations: DOPC, 1,2-dioleoyl-*sn*-glycero-3-phosphocholine; IBA, 3-indolebutyric acid; TPC, 1,2-dioleoyl-*sn*-glycero-3-phosphotempocholine; 5SLPC, 1-palmitoyl-2-(5-doxyl)stearoylphosphatidylcholine; 12SLPC, 1-palmitoyl-2-(12-doxyl)stearoylphosphatidylcholine; MLV, multilamellar vesicle(s); SUV, small unilamellar vesicle(s).

this study, with the exception of IBA and 11-CU, do not have ionizable groups in the range of pH 5–8, and therefore the results are applicable to a physiological pH of 7.4. To prepare MLV, samples were dried with  $N_2$ , remixed in  $CHCl_3$ , and then redried with  $N_2$ . Due to fluorophore sublimation problems, samples were not further dried under high vacuum. Samples were then resuspended in 1 mL of the buffers used above.

**Steady-State Fluorescence Measurements.** Fluorescence was measured on a Spex 212 Fluorolog spectrofluorometer using semimicro quartz cuvettes. Unless otherwise noted, the excitation/emission wavelengths used were 289 nm/359 nm for carbazole, 292 nm/368 nm for 9-methylcarbazole, 280 nm/360 nm for IBA, 355 nm/402 nm for anthracene, 365 nm/415 nm for 9-methylanthracene, and 270 nm/310 nm for 4-(*tert*-octyl)phenol. Background fluorescence in samples lacking fluorophore was subtracted.

The distance of the fluorophores from the center of the bilayer ( $Z_{cf}$ ) was calculated using the parallax equation (Chattopadhyay & London, 1987; Abrams & London, 1993):  $Z_{cf} = L_{c1} + (-[\ln(F_1/F_2)/\pi C] - L_{21}^2)/2L_{21}$ , where  $F_1$  and  $F_2$  are the fluorescence intensity in the presence of a shallow and deeper nitroxide, respectively,  $L_{c1}$  is the distance of the shallow nitroxide from the bilayer center,  $L_{21}$  is the distance between shallow and deep quenchers, and  $C$  is the quencher concentration in molecules per angstrom squared. The distances of the nitroxides from the center of the bilayer are 19.5 Å for TPC, 12.15 Å for 5SLPC, and 5.85 Å for 12SLPC (Abrams & London, 1993). To calculate  $Z_{cf}$ , the pair of nitroxide labels which quenched the greatest were used (Abrams & London, 1993), except for IBA in MLV, where the weakest quenching  $F/F_0$  values were within 5%,  $0.95 < F_1/F_2 < 1.05$  (see Table 1). In this case, the depth was calculated from an average of the two most strongly quenching pairs.

**Acrylamide Quenching of Carbazole Probes.** Acrylamide quenching experiments were carried out using SUV-bound fluorophore. Samples were prepared as described above, keeping the DOPC concentration at 200  $\mu$ M. Experiments at pH 10 were performed in a buffer of 10 mM glycine, 150 mM NaCl. Small aliquots of 3.9 M acrylamide/water were titrated into the samples, and fluorescence intensities were acquired after 1 and 3 min to ensure equilibration. Osmotic shrinking experiments (London & Feigenson, 1981) demonstrated acrylamide is able to permeate into the aqueous lumen of the vesicles rapidly (data not shown), and no incubation time dependence of quenching was observed. Excitation wavelengths, 298 nm for carbazole and 300 nm for 9-methylcarbazole (11-CU, pH 5 and pH 10), were chosen such that inner filter effects would be avoided (UV absorbance of 100 mM acrylamide at 298 nm is approximately 0.01). Emission intensities were measured near  $\lambda_{max}$ , at 360 nm for carbazole, 368 nm for 9-methylcarbazole, and 367 nm for 11-(9-carbazole)undecanoate at pH 5 and 10. Fluorescence intensities were corrected for dilution.  $K_{sv}$  values were calculated from the data as described in Table 2.

To determine whether carbazole exchange between membrane-bound and membrane-free forms is rapid, the same experiments were repeated for 9-methylcarbazole in the presence of 100  $\mu$ M DOPC. The predicted quenching of carbazole for the case of slow exchange was calculated from the modified Stern–Volmer equation:  $F_0/F = 1/[F_b\{1/(1 +$

$K_{svb}[Q])\} + F_a\{1/(1 + K_{sva}[Q])\}]$  where  $F_0$  and  $F$  are the fluorescence intensities in the absence and presence of quencher, respectively, and  $[Q]$  is the acrylamide concentration.  $F_b$  and  $F_a$  are the fraction of fluorescence intensities from the membrane-bound and unbound species, respectively, and  $K_{svb}$  and  $K_{sva}$  are their respective Stern–Volmer constants from Table 2. The predicted quenching for fast exchange was calculated from the Stern–Volmer equation, replacing  $K_{sv}$  with  $K_{sv}(\text{average}) = K_{svb}(\text{fraction of 9-methylcarbazole membrane-bound}) + K_{sva}(1 - \text{fraction of 9-methylcarbazole bound})$ . The fraction of 9-methylcarbazole that was membrane-bound, and  $F_b$ , and  $F_a$  were derived from a binding curve obtained from the increase in 9-methylcarbazole fluorescence upon addition of lipid vesicles. This curve gave a  $K_d$  apparent of about 110  $\mu$ M (data not shown). The fraction of bound 9-methylcarbazole at 100  $\mu$ M DOPC was then calculated from (fluorescence at 100  $\mu$ M DOPC – fluorescence at 0  $\mu$ M DOPC)/(maximum fluorescence at high DOPC concentration – fluorescence at 0  $\mu$ M DOPC);  $F_a$  was calculated from (fluorescence at 0  $\mu$ M DOPC)/(fraction of carbazole unbound at 100  $\mu$ M DOPC)/(total fluorescence at 100  $\mu$ M DOPC);  $F_b = 1 - F_a$ .

**Lifetime Measurements.** SUV samples were similarly prepared as described above except that 4  $\mu$ M fluorophore was suspended in 400  $\mu$ M DOPC. Lifetimes were determined using a Spex  $\tau 2$  spectrofluorometer. The excitation wavelength was 291 nm for 11-CU, pH 5 and 10, and 292 nm for carbazole and 9-methylcarbazole. Emission was measured at 358 nm for carbazole, 368 nm for 9-methylcarbazole, and 369 nm for 11-(9-carbazole)undecanoate. A glycogen light scattering standard was used (Lakowicz, 1983). Eight to ten modulation frequencies between 4 and 80 MHz were used. Lifetimes shown are for modulation and phase data fit to a discrete value, which generally gave  $\chi^2$  of 1–2 using a phase error of 0.6° and a modulation error of 0.006. Due to a relatively weak signal, no attempt was made to analyze lifetime data with more complex models. Duplicate  $\tau$  measurements were within 0.1–0.4 ns of each other.

## RESULTS AND DISCUSSION

The membrane depths of Trp, Tyr, indole, and phenol by themselves could not be examined due to their relatively weak binding to model membranes. Therefore, fluorescent probes were chosen that retain the essential structural features of these groups, but bind to bilayers more tightly.<sup>2</sup> Octylphenol was chosen as a Tyr analog. 3-Indolebutyric acid (IBA) and carbazole derivatives were used as analogs for Trp residues. Carbazoles resemble indoles but contain an extra phenyl ring. The availability of a series of carbazoles was particularly useful for dissecting various structural contributions to membrane depth.

The Trp and Tyr analogs were incorporated into multilamellar vesicles (MLV) or small unilamellar vesicles (SUV) containing nitroxide-labeled phospholipids, and then the

<sup>2</sup> The binding of probes to bilayers was measured through the increase in their fluorescence intensity upon binding (data not shown). All of the compounds showed half-maximal increases in the range 50–150  $\mu$ M phospholipid, and combining this with the intensity increase upon binding to bilayers allows estimation that at least 95% of fluorescence arises from membrane-bound fluorophore at 200  $\mu$ M phospholipid, except in the case of IBA (see Table 1).

Table 1: Nitroxide Quenching and Depth of Fluorophores

fluorophore	vesicle	$F/F_0^a$			$Z_{cf}^{MLV/SUV^b}$ (Å)	$Z_{cf}^b$ (Å)
		$F_{TPC}/F_0$	$F_{5SLPC}/F_0$	$F_{12SLPC}/F_0$		
carbazole	MLV	0.461	0.431	0.519	15.1	$15.2 \pm 0.2$
	SUV	0.458	0.432	0.514	15.2	
9-methylcarbazole	MLV	0.463	0.407	0.552	13.7	$13.6 \pm 1.6$
	SUV	0.399	0.340	0.422	13.4	
11-( <i>N</i> -carbazole)undecanoic acid						
pH 5 <sup>c</sup>	MLV	0.442	0.324	0.286	7.5	(7.5)
pH 10 <sup>c</sup>	MLV	0.369	0.287	0.329	10.6	(10.6)
3-indolebutyric acid <sup>d</sup>	MLV	0.564	0.521	0.584	12.8	$14.5 \pm 1.6$
	SUV	0.621	0.613	0.667	15.7	
anthracene	MLV	0.479	0.321	0.383	11.1	$10.3 \pm 1.1$
	SUV	0.491	0.336	0.360	9.9	
9-methylanthracene	MLV	0.309	0.213	0.212	9.0	$9.2 \pm 0.7$
	SUV	0.298	0.199	0.205	9.4	
4-( <i>tert</i> -octyl)phenol	MLV	0.306	0.258	0.405	14.1	$13.8 \pm 0.8$
	SUV	0.312	0.270	0.385	13.7	

<sup>a</sup>  $F/F_0$  is the ratio of fluorescence intensity in samples composed of 85 mol % DOPC and 15 mol % TPC, 5SLPC, or 12SLPC to fluorescence intensity in DOPC vesicles. <sup>b</sup>  $Z_{cf}^{MLV/SUV}$  is the distance of the fluorophore from the bilayer center in MLV or SUV as indicated at the left.  $Z_{cf}$  is the average of several individual SUV and MLV results, and standard deviations are shown for 3–6 experiments each using duplicate or triplicate samples. <sup>c</sup> 11-CU examined at pH 5 and pH 10 to determine the shift in depth due to the protonated and ionized species. Data from Abrams and London (1992). <sup>d</sup> Uncorrected for IBA in aqueous solution. Corrected values calculated after estimation of the fraction of IBA fluorescence from solution (20%, see Materials and Methods) gave  $Z_{cf} = 14.3$  Å.

amount of quenching induced by phospholipids with a nitroxide in a shallow (TPC), medium (5SLPC), or deep (12SLPC) location in the bilayer was measured. The amount of quenching is given by the parameter  $F/F_0$ , the ratio of fluorescence in vesicles containing quencher to that in vesicles lacking quencher.  $F/F_0$  values in Table 1 show that all of the nitroxide-labeled lipids are able to quench fluorescence to different extents.

The distances of the fluorophores from the center of the bilayer were then calculated from the differences in quenching by the nitroxide-labeled lipids using the parallax equation (see Materials and Methods). The results are summarized in Table 1, and illustrated schematically in Figure 3. Table 1 shows that for each fluorescent probe, the location in SUV was the same as the location in MLV (with the possible exception of the indole in IBA). More importantly, Table 1 also shows carbazole, 9-methylcarbazole, indole, and phenol groups are located about 14–15 Å from the bilayer center. This is close to the depth of the ester groups on phospholipids (Weiner & White, 1992), and represents the polar–hydrocarbon boundary. In addition, Table 1 shows this depth is 4–5 Å shallower than that occupied by anthracene and 9-methylanthracene. Therefore, indole and phenol analogs seek out a shallower location than ordinary aromatic hydrocarbons.

In contrast, previous studies (Abrams & London, 1992) have found the *N*-substituted carbazole group in 11-(9-carbazole)undecanoic acid does not occupy a shallow location in the membrane (Table 1). Presumably, the tendency of the undecanoic acyl chain to align with the acyl chains of the lipids overcomes the tendency of the carbazole to seek a polar location. A similar effect has been seen for anthroxyl probes, which occupy a deep location only when attached to acyl chains (Waggoner & Stryer, 1970; Abrams & London, 1993).

To check the carbazole locations determined by nitroxide quenching, acrylamide quenching was performed. Acrylamide is a polar molecule used to conduct quenching experiments in aqueous solution (Eftink & Ghiron, 1981). Quenching by acrylamide is much less for fluorophores

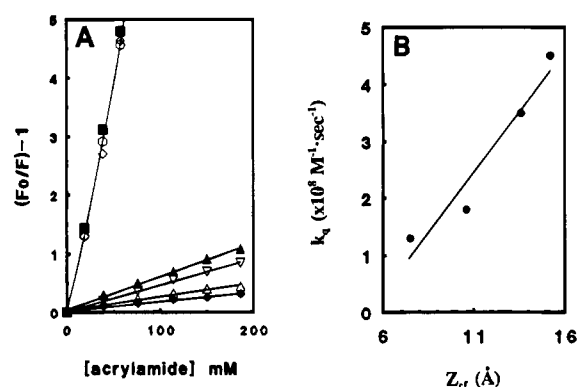


FIGURE 1: Acrylamide quenching of carbazole probes. (A) Effect of acrylamide concentration on quenching. Quenching is shown for (▲) carbazole/DOPC, pH 5; (▽) 9-methylcarbazole/DOPC, pH 5; (Δ) 11-(9-carbazole)undecanoate/DOPC, pH 10; (◆) 11-(9-carbazole)undecanoate/DOPC, pH 5; (■) carbazole in pH 5 buffer; (○) 9-methylcarbazole in pH 5 buffer; (◇) 11-(9-carbazole)undecanoate in pH 10 buffer. Data shown are the average of two experiments. (B) Correlation of  $k_q$  with  $z_{cf}$  for model membrane-bound carbazole probes.  $k_q$  and  $z_{cf}$  values were obtained from Tables 1 and 2.

Table 2: Quenching of Carbazoles by Acrylamide

fluorophore	$K_{sv}^a$ (M <sup>-1</sup> )	$\tau_0$ (ns)	$k_q$ ( $\times 10^9$ ) (M <sup>-1</sup> s <sup>-1</sup> )
carbazole, pH 5	91	10.5	8.7
9-methylcarbazole, pH 5	86	9.9	8.7
11-(9-carbazole)undecanoate, pH 10	84	9.9	8.5
carbazole/DOPC, pH 5	5.8	13.0	0.45
9-methylcarbazole/DOPC, pH 5	4.6	13.3	0.35
11-(9-carbazole)undecanoate acid/ DOPC, pH 10	2.5	13.5	0.18
11-(9-carbazole)undecanoic acid/ DOPC, pH 5	1.7	13.6	0.13

<sup>a</sup>  $K_{sv}$  and  $k_q$  were calculated from the initial slopes of the data in Figure 1, and the Stern–Volmer equation:  $F_0/F = 1 + K_{sv}[Q] = 1 + k_q\tau_0[Q]$ .

buried in the bilayer (Bolen & Holloway, 1990). Acrylamide quenching of carbazoles is shown in Figure 1A.  $k_q$  values calculated from these data using the Stern–Volmer equation

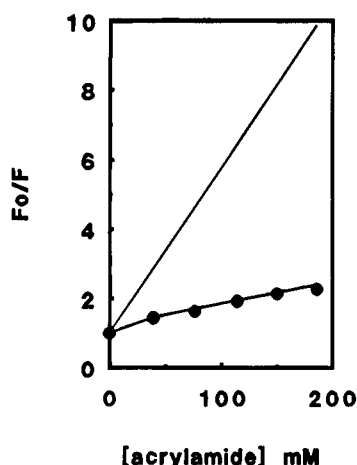


FIGURE 2: Quenching of 9-methylcarbazole partly bound to model membrane vesicles demonstrates slow carbazole exchange. The predicted quenching for a mixture of membrane-bound and aqueous 9-methylcarbazole in the presence of 100  $\mu$ M DOPC is shown for models in which the exchange rate of bound and free carbazole is fast (upper curve) or slow (lower curve) relative to the excited state lifetime. See Materials and Methods for the calculation of quenching predicted for fast and slow exchange rates.

and fluorescence lifetime measurements are summarized in Table 2.  $k_q$ , the rate constant for quenching, largely reflects the number of collisions between acrylamide and carbazole, and should decrease progressively with increased depth. There is a strong correlation between  $k_q$  and  $z_{cf}$ , consistent with the depths obtained from nitroxide quenching (Figure 1B).

To rule out that carbazole  $k_q$  might reflect quenching during periods of fluorophore dissociation from the bilayer rather than fluorophore depth, the exchange of a carbazole derivative between membrane-bound and aqueous locations was examined. As shown in Figure 2, the quenching obtained only fits a model where membrane-bound carbazoles do not dissociate during their excited state lifetime.

Another concern is that the  $z_{cf}$  values might be influenced by a change in fluorophore location in the excited state. Increased polarity in the excited state might cause a membrane-inserted fluorophore deeply buried in the ground state to move to a polar location after excitation. [This is

not of concern for phenol for which polarity does not increase significantly in the excited state (Demchenko, 1986).] Given the low diffusion coefficient in membranes (Gennis, 1989), there appears to be insufficient time for much motion during the excited state lifetimes of the probes used in this study (calculation not shown). In addition, we have previously observed in molecules that move toward the surface in the excited state, including a 11-(9-carbazole)undecanoic acid derivative, there is a dependence of depth on emission wavelength (Abrams et al., 1992; Abrams & London 1993), but none was detected for methylcarbazole or carbazole (not shown).

Because the charge on a fluorophore could influence its location, a change in the ionization state of a fluorophore in the excited state is an additional concern. In particular, excited state phenols ionize at a much lower pH than in the ground state (Barlthrop & Coyle, 1978). However, even for a diffusion-controlled reaction the excited state phenol  $pK_a$  of 5 (Barlthrop & Coyle, 1978) implies a  $k_{\text{proton dissociation}}$  (Jencks, 1969) too slow to allow a proton loss during the excited state lifetime (3.6 ns; Demchenko, 1986). Supporting this conclusion, bilayer-inserted octylphenol gave an emission spectrum corresponding to that of the protonated phenol ( $\lambda_{\text{max}}$  305 nm), rather than the ionized form ( $\lambda_{\text{max}}$  340 nm) (data not shown).

An important question is why indole, carbazole, and phenol groups locate at the polar–hydrocarbon boundary. Hydrogen bonding by the indole NH (Wimley & White, 1992, 1993) and phenol OH is likely to contribute to the localization at the polar–hydrocarbon boundary, where the concentration of water and other hydrogen bonding groups is much greater than in the acyl chain hydrocarbon region of the bilayer. However, in agreement with the observations of Wimley and White (1992, 1993), the shallow depth of N-substituted methylcarbazole, which lacks the ability to hydrogen bond, shows hydrogen bonding is not the sole determinant of shallow location, and the polarity due to the presence of a nitrogen atom appears to be sufficient to account for methylcarbazole location. Nevertheless, the 1.5 Å deeper location of 9-methylcarbazole relative to carbazole suggests hydrogen bonding or the methyl group itself influences depth.

A contribution of aromatic structure to a shallow depth also cannot be ruled out. It is noteworthy that the depths of

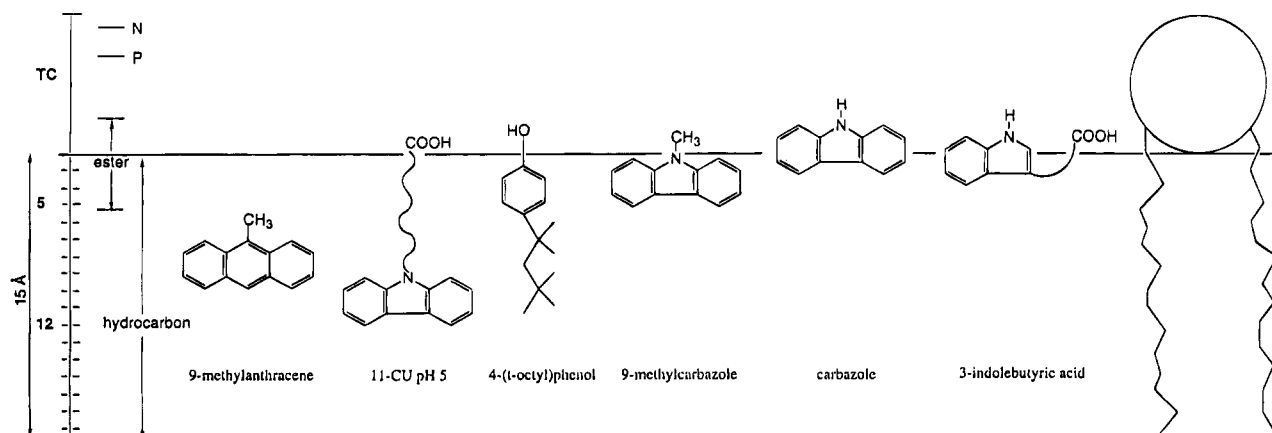


FIGURE 3: Schematic illustration of the location of Trp and Tyr analogs in lipid bilayers. The center of the molecules is shown at  $z_{cf}$ . For comparison, the location of the functional groups of a phospholipid, as estimated in the study of Weiner and White (1992), as well as the nitroxide depth for the quenchers used (Abrams & London, 1993) is shown on the left. The upper solid line delineates the approximate polar/hydrocarbon boundary 15 Å from the bilayer center. 11-CU is 11-(9-carbazole)undecanoic acid.

the anthracenes given in Table 1 are slightly shallower than might be predicted for a hydrocarbon randomly distributed in the acyl chain region of the bilayer.

The localization of indoles and phenols near a polar region is supported by a number of other studies. Wimley and White (1992, 1993) inferred that indole and *N*-methylindole only undergo partial burial in the hydrocarbon region of bilayers based on binding studies. Although they did not specify exact depths for these groups, it is noteworthy that the slightly deeper degree of "burial" they found for *N*-methylindole relative to indole (Wimley & White, 1993) parallels the slightly deeper location of *N*-methylcarbazole relative to carbazole observed in this study. In addition, the depths found for Trp and Tyr analogs in this study show a close correspondence to the depth of Trp and Tyr residues in the photosynthetic reaction center (Deisenhofer & Michel, 1989), porin (Weiss et al., 1991; Schabert et al., 1995), and in proteins with single transmembrane helices<sup>3</sup> (Landolt-Marticorena et al., 1993). This lends strong support to the suggestion that these residues play an important role in anchoring membrane proteins at precise locations in the bilayer (Schiffer et al., 1992). Even a small change in depth might be unfavorable in proteins anchored by these residues, and the number of Trp and Tyr residues in a membrane protein may help regulate the amount of protein displacement perpendicular to the plane of the membrane such that a protein with many Tyr and Trp residues may remain more precisely aligned with the polar and hydrocarbon groups on lipids.

Finally, it should be noted that the agreement of the nitroxide-determined depths obtained in this study with the acrylamide quenching results and the other studies noted above further confirms the reliability of nitroxide-quenching determined depths. Additional studies using this method to relate molecular structure to membrane location should yield further insights into the localization of biomolecules in membranes.

<sup>3</sup> The fact that shallow depths were found for analogs that are more hydrophobic than ordinary indole and phenol strengthens the conclusion that Trp and Tyr would prefer shallow depths. At most, indole and phenol themselves may occupy slightly shallower locations than measured for the probes in this study.

## REFERENCES

- Abrams, F. S., & London, E. (1992) *Biochemistry* 31, 5312–5322.  
 Abrams, F. S., & London, E. (1993) *Biochemistry* 32, 10826–10831.  
 Abrams, F. S., Chattopadhyay, A., & London, E. (1992) *Biochemistry* 31, 5322–5327.  
 Asuncion-Punzalan, E., & London, E. (1995) *Biochemistry* 34, 11460–11466.  
 Barltrop, J. A., & Coyle, J. D. (1978) *Principles of Photochemistry*, pp 50–51, J. Wiley and Sons, New York.  
 Bolen, E. J., & Holloway, P. W. (1990) *Biochemistry* 29, 9638–9643.  
 Chattopadhyay, A., & London, E. (1987) *Biochemistry* 26, 39–45.  
 Chung, L. A., Lear, J. D., & DeGrado, W. F. (1992) *Biochemistry* 31, 6608–6616.  
 Deisenhofer, J., & Michel, H. (1989) *Science* 245, 1463–1473.  
 Demchenko, A. P. (1986) *Ultraviolet Spectroscopy of Proteins*, pp 23–53, Springer-Verlag, New York.  
 Eftink, M. R., & Ghiron, C. A. (1981) *Anal. Biochem* 114, 199–227.  
 Gennis, R. B. (1989) *Biomembranes*, p 183, Springer-Verlag, New York.  
 Jencks, W. P. (1969) *Catalysis in Chemistry and Enzymology*, pp 209–210, McGraw-Hill, New York.  
 Jones, J. D., & Gierasch, L. M. (1994) *Biophys. J.* 67, 1534–1545.  
 Lakowicz, J. R. (1983) *Principles of Fluorescence Spectroscopy*, p 86, Plenum, New York.  
 Landolt-Marticorena, C., Williams, K. A., Deber, C. M., & Reithmeier, R. A. F. (1993) *J. Mol. Biol.* 229, 602–608.  
 London, E., & Feigenson, G. W. (1981) *Biochemistry* 20, 1932–1938.  
 Matsuzaki, K., Murase, O., Tokuda, H., Funakoshi, S., Fujii, N., & Miyajima, K. (1994) *Biochemistry* 33, 3342–3349.  
 Palmer, L. R., & Merrill, A. R. (1994) *J. Biol. Chem.* 269, 4187–4193.  
 Rodionova, N. A., Tatulian, S. A., Surrey, T., Jahnig, F., & Tamm, L. (1995) *Biochemistry* 34, 1921–1929.  
 Schabert, F. A., Henn, C., & Engel, A. (1995) *Science* 268, 92–94.  
 Schiffer, M., Chang, C. H., & Stevens, F. J. (1992) *Protein Eng.* 5, 213–214.  
 Waggoner, A. S., & Stryer, L. (1970) *Proc. Natl. Acad. Sci. U.S.A.* 67, 579–589.  
 Weiss, M. S., Abele, U., Weckesser, J., Welte, W., Schiltz, E., & Schulz, G. E. (1991) *Science* 254, 1627–1630.  
 Wiener, M. C., & White, S. H. (1992) *Biophys. J.* 61, 434–447.  
 Wimley, W. C., & White, S. H. (1992) *Biochemistry* 31, 12813–12818.  
 Wimley, W. C., & White, S. H. (1993) *Biochemistry* 32, 6307–6312.

BI951832Q